JACS
JOURNAL OF THE AMERICAN CHEMICAL SOCIETY

Communication

pubs.acs.org/JACS

Aggregation of Individual Sensing Units for Signal Accumulation: Conversion of Liquid-Phase Colorimetric Assay into Enhanced Surface-Tethered Electrochemical Analysis

Tianxiang Wei, Tingting Dong, Zhaoyin Wang, Jianchun Bao, Wenwen Tu, and Zhihui Dai*

Jiangsu Collaborative Innovation Centre of Biomedical Functional Materials and Jiangsu Key Laboratory of Biofunctional Materials, School of Chemistry and Materials Science, Nanjing Normal University, Nanjing 210023, P. R. China

Supporting Information

ABSTRACT: A novel concept is proposed for converting liquid-phase colorimetric assay into enhanced surface-tethered electrochemical analysis, which is based on the analyte-induced formation of a network architecture of metal nanoparticles (MNs). In a proof-of-concept trial, thymine-functionalized silver nanoparticle (Ag-T) is designed as the sensing unit for Hg^{2+} determination. Through a specific T-Hg^{2+}-T coordination, the validation system based on functionalized sensing units not only can perform well in a colorimetric Hg^{2+} assay, but also can be developed into a more sensitive and stable electrochemical Hg^{2+} sensor. In electrochemical analysis, the simple principle of analyte-induced aggregation of MNs can be used as a dual signal amplification strategy for significantly improving the detection sensitivity. More importantly, those numerous and diverse colorimetric assays that rely on the target-induced aggregation of MNs can be augmented to satisfy the ambitious demands of sensitive analysis by converting them into electrochemical assays via this approach.

Numerous types of liquid-phase colorimetric assays have been developed via localized surface plasmon resonance changes of metal nanoparticles (MNs).[1] These assays are based on target-recognition-induced aggregation of MNs and have been applied in various fields, such as environmental monitoring,[2,3] disease diagnostics,[4−7] and food analysis.[8,9] Among their superior features, the most prominent are their simple manipulation principle and easy procedures for signal readout, which render them suitable for on-site or point-of-care testing.[10−13] However, the majority of colorimetric assays exhibit poor sensitivity. Therefore, it is highly desirable to design a more sensitive method to meet the current demand.

Previous reports have brought new ideas to us. For example, when infrared radiation (a well-known technique in physics) was transferred into the field of clinical medicine, lots of exciting medical treatments and diagnostic techniques emerged.[14] Similarly, through exchanging fluorescence probes for redox-active Fc-deoxyuridine triphosphate markers, Hsing et al. developed a new technique combining the real-time polymerase chain reaction with electrochemistry, which has been used for the real-time monitoring of nucleic acids with decreased assay time and cross-contamination.[15] In short, the above examples are re-creations of the existing platforms for achieving new goals, simply infusing one principle or technique into another field, yet producing brand new achievements. Therefore, in comparison with MNs-based colorimetric assays, we expect that electrochemical analysis can be adapted from these assays in several aspects. First, the self-sensitive electrochemical methods, like anodic stripping voltammetry and linear-sweep voltammetry (LSV), are powerful tools for the characterization of trace metal ions or MNs.[16−18] Therefore, MNs can be readily used as electrochemical probes to provide a well-defined electrochemical signal. Second, a single modification strategy can be utilized for both assays. The functionalization of MNs with sensing elements is a key procedure in MN-based colorimetric detection. Metal electrodes, especially gold electrodes, exhibit a superficial microenvironment similar to that of MNs. Thus, the functionalization procedure can be directly employed for electrode modification. The target-induced aggregation of MNs in a solution can be facilely initiated on a solid (electrode)−liquid (electrolyte) surface. Additionally, increasing amounts of MNs are gathered onto the electrode surface through target induction, which significantly amplifies the signal response and further improves sensitivity. On the basis of the three aforementioned aspects, a general method is first put forward for converting liquid-phase colorimetric assays into a more sensitive surface-tethered electrochemical analysis.

The perniciousness of Hg^{2+} contamination in food, water, and the environment has become a serious public health concern.[19,20] Herein, using Hg^{2+} determination as a model, proof-of-concept verification experiments were designed and conducted to demonstrate the improved electrochemical assay that was adapted from an MN-based colorimetric assay. In particular, two types of Hg^{2+} sensors were developed, i.e., colorimetric and electrochemical sensors, both employing the same modified metal nanoprobe (a thymine-functionalized silver nanoparticle (Ag-T) nanoprobe) as the sensing unit. The procedure for the synthesis of sensing probes is illustrated in Figure 1. The Ag nanoparticles (NPs) were synthesized and purified according to methods previously reported, with minor modifications[21] (for details, see the Supporting Information (SI)), and then the surface of the Ag NPs was modified with cysteamine. The cysteamine-modified Ag NPs (Ag-cys) were further functionalized with thymine-1-acetic acid (T-COOH)

Received: April 27, 2015
Published: July 6, 2015

DOI: 10.1021/jacs.5b04348
J. Am. Chem. Soc. 2015, 137, 8880−8883

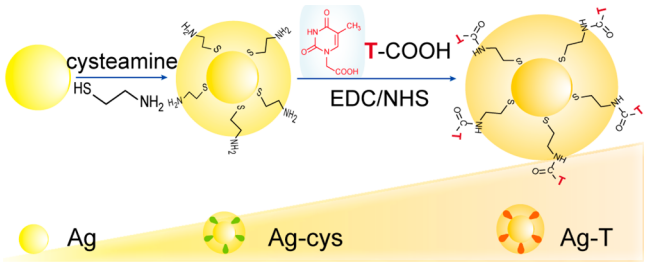

Figure 1. Schematic representation of the formation of an Ag-T sensing unit.

using the *N*-(3-(dimethylamino)propyl)-*N*′-ethylcarbodiimide hydrochloride crystalline (EDC)/*N*-hydroxysuccinimide (NHS) strategy. Notably, the thymine in thymidine plays a pivotal role in the coordination of highly specific T-Hg^{2+}-T; thus, thymine itself (instead of thymidine or thymidine-containing oligonucleotides) may be a superior sensing element for the quantification of Hg^{2+} ions. In this work, we used thymine-functionalized MNs for Hg^{2+} detection.

Transmission electron microscopy (TEM) images of Ag NPs, Ag-T nanoprobes, and Hg^{2+}-induced accumulation of Ag-T units are shown in Figure 2A–C, respectively. According to

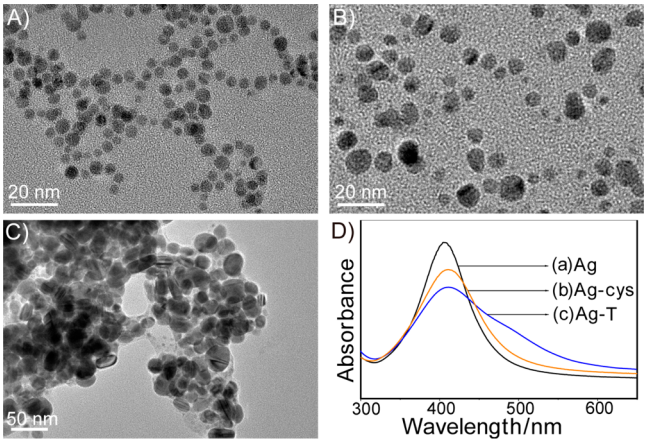

Figure 2. TEM images of (A) Ag NPs, (B) Ag-T nanoprobes in the absence of Hg^{2+} ions, and (C) accumulation of Ag-T nanoprobes in the presence of 100 nM Hg^{2+} ions. (D) UV–vis spectra of (a) Ag NPs, (b) Ag-cys, and (c) Ag-T.

the distinct behavior of the Ag-T nanoprobes in the absence and presence of 100 nM Hg^{2+} ions (Figure 2B,C), thymine on the surface of Ag NPs can adsorb Hg^{2+} ions, resulting in obvious aggregation of the Ag-T nanoprobes. Dynamic light scattering analysis showed distinct changes of the average hydrodynamic sizes from about 15 nm to about 300 nm after addition of Hg^{2+} ions (SI, Figure S1). The synthesized Ag-T nanoprobe was also characterized via UV–visible spectroscopy. As shown in Figure 2D, Ag-cys exhibited a red shift of the absorption peak and a broader absorption band than unmodified Ag NPs (curves a and b). The covalent linkage of T-COOH further broadened the absorption band (curve c). These observations are consistent with the effect of surface molecules on MNs,[22] suggesting the successful formation of an Ag-T nanoprobe.

Liquid-phase colorimetric Hg^{2+} sensing was first performed by using the Ag-T sensing units. Hg^{2+} determination was achieved via the color change of the Ag-T system. As shown in Figure 3A, with the increased concentration of Hg^{2+} ions in the presence of the Ag-T nanoprobes, the color of the mixed

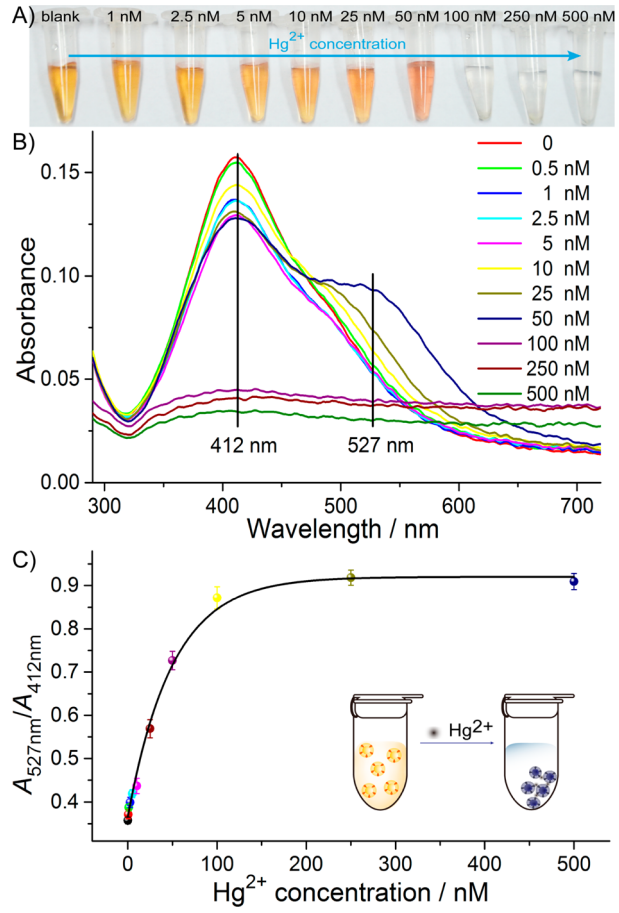

Figure 3. (A) Photograph showing the color change of the Ag-T nanoprobe upon the addition of different concentrations of Hg^{2+} ions. (B) UV–vis absorption spectra of the Ag-T nanoprobe with different concentrations of Hg^{2+} ions. (C) Calibration curve for $A_{527\ nm}/A_{412\ nm}$ value versus Hg^{2+} concentrations. Inset: Illustration of a colorimetric Hg^{2+} sensor with Ag-T nanoprobes.

solution gradually changed from goldenrod to copper and then to blue-gray. Corresponding UV–vis spectra were collected to reflect the color change more accurately (Figure 3B). The extinction peaks in the UV–vis spectra at 412 and 527 nm represented the dispersed and aggregated Ag-T nanoprobes, respectively. Accordingly, the ratio of $A_{527\ nm}/A_{412\ nm}$ was used to quantify Hg^{2+}-induced aggregation in this work (Figure 3C). The obtained detection range of this colorimetric Hg^{2+} sensor was 0.5–100 nM, which covers the maximum level for Hg^{2+} ions in drinking water permitted by the European Union (5 nM) and the maximum level permitted by the U.S. Environmental Protection Agency (10 nM).[23] This sensor was also challenged with 5 μM amounts of other metal ions (including Cr^{3+}, Ni^{2+}, Co^{2+}, Pb^{2+}, Cd^{2+}, Zn^{2+}, Fe^{3+}, K^{+}, Na^{+}, Ca^{2+}, Mg^{2+}, and Ag^{+}) to examine its selectivity (SI, Figure S2). The acceptable sensitivity and good selectivity of the colorimetric Hg^{2+} sensor indicated its potential application in real samples.

To improve the sensitivity of this colorimetric Hg^{2+} sensor, we transferred it to an electrochemical Hg^{2+} sensor that was also constructed by using the Ag-T nanoprobe. According to the design (Figure 4A), a thymine-monolayer-modified gold electrode (Au-T) could capture Hg^{2+} ions and Ag-T nanop-

DOI: 10.1021/jacs.5b04348
J. Am. Chem. Soc. 2015, 137, 8880–8883

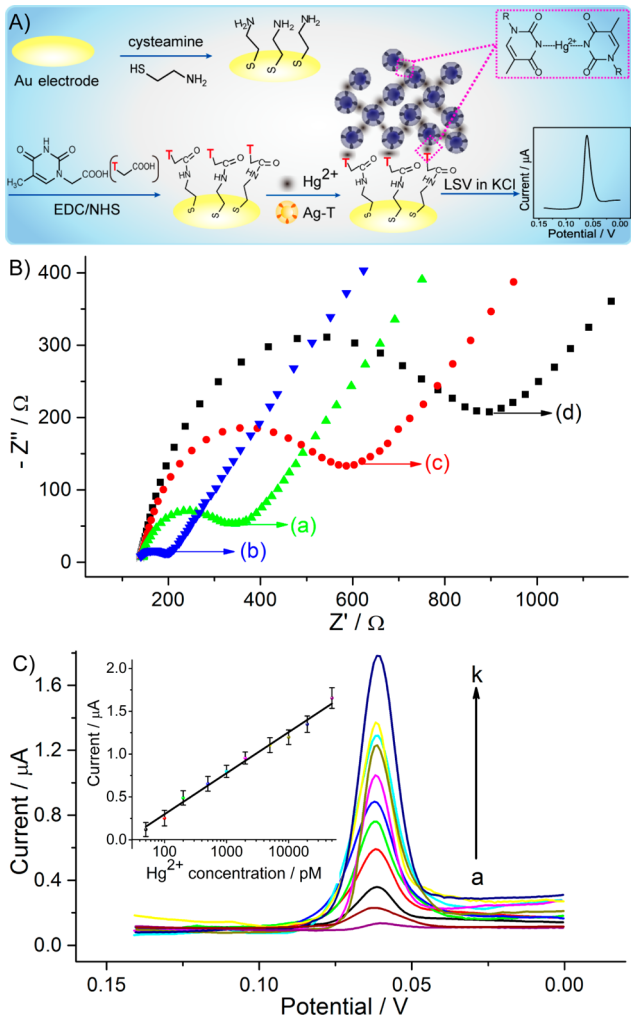

Figure 4. (A) Illustration of an electrochemical Hg^{2+} sensor based on Ag-T nanoprobes. (B) Nyquist plots for the different electrodes of (a) Au, (b) Au-cys, (c) Au-T, and (d) Au-T incubated with Ag-T nanoprobes in the presence of 5 nM Hg^{2+} ions. (C) LSV curves for the Ag-T-based nanostructure formed with different concentrations of Hg^{2+} ions (a–k representing 0, 0.05, 0.1, 0.2, 0.5, 1.0, 2.0, 5.0, 10, 20, and 50 nM Hg^{2+} ions, respectively). Inset: Calibration curve for the current value vs the Hg^{2+} concentrations.

robes through T-Hg^{2+}-T coordination. Surface-tethered Ag-T nanoprobes can recruit more Hg^{2+} ions as well as other Ag-T nanoprobes, resulting in the formation of an Ag-T-Hg^{2+}-T-Ag architecture on the electrode surface. Hg^{2+} ions trigger the formation of an Ag-T-based nanostructure. Hg^{2+} quantification can thus be analyzed using the amplified electrochemical signal of Ag NPs.[21,24,25] To ensure that plenty of Hg^{2+} ions are absorbed onto Au-T, a sequential procedure was adopted in fabricating the sensing system, i.e., the two-step method as described in the SI: the Au-T was incubated first with Hg^{2+} ions for a certain time, and then Ag-T was added to continue the reaction. Compared with the sensing system fabricated via the one-step method (incubating Au-T directly in a mixture of Hg^{2+} ions and Ag-T), a larger response was obtained via the two-step method (SI, Figures S3). The results indicated that the sequential procedure that we adopted could effectively reduce the potential competition for adsorption between Ag-T nanoprobes and Au-T surface.

The procedure for fabricating the electrochemical Hg^{2+} sensor was investigated via electrochemical impedance spectroscopy, which was widely used to characterize molecular assembly on electrode surfaces. Compared with the diameter of the semicircle in the impedance spectrum of the bare Au electrode (curve a in Figure 4B), the diameter of the semicircle in the impedance spectrum of the cysteamine-modified electrode (Au-cys) decreased (curve b). The decreased semicircle diameter may indicate that the positively charged self-assembled monolayer of cysteamine attracted the negatively charged redox-active probe ($[Fe(CN)_6]^{3-/4-}$) onto the electrode surface, which may have decreased the electron transfer resistance.[26] After the electrode was modified with thymine, the semicircle diameter increased (curve c), suggesting increased electron transfer resistance. After the Au-T was incubated with the Ag-T nanoprobes in the presence of Hg^{2+} ions, the electrochemical impedance of the electrode further increased (curve d), which is attributed to the repellent property of the Ag-T-Hg^{2+}-T-Ag network architecture against $[Fe(CN)_6]^{3-/4-}$. Scanning electron microscopy images also confirmed the formation of an Ag-T-Hg^{2+}-T-Ag network architecture on the electrode surface (SI, Figure S4). Moreover, 10 nM Hg^{2+} ions and Ag-T nanoprobes were used to treat the Au-T. After the electrode was removed from the test solution, the solution was subsequently analyzed via inductively coupled plasma mass spectrometry (ICP-MS) for Hg^{2+} quantitation. The amounts of Hg^{2+} ions in the treated solutions were 2.8, 2.6, and 3.1 nM, respectively. The results revealed that most of the Hg^{2+} ions had been transferred onto the electrode surface, which was ascribed to the formation of the Ag-T-Hg^{2+}-T-Ag network architecture.

LSV was used to investigate the feasibility of the electrochemical Hg^{2+} sensor. As shown in SI, Figure S5, a very small signal was recorded in the absence of Hg^{2+} ions (green curve). In contrast, a large and well-defined electrochemical signal was recorded in the presence of Hg^{2+} ions (red curve). These results verified that Ag-T nanoprobe-based Hg^{2+} detection can be achieved using the electrochemical method.

Under optimized measurement conditions (SI, Figure S6), the Hg^{2+} quantitative assay was conducted by monitoring the LSV responses of the Ag NPs in the Ag-T-Hg^{2+}-T-Ag network architecture formed on the electrode surface. As shown in Figure 4C, the LSV peak current (I) increased with increasing Hg^{2+} concentration ($[Hg^{2+}]$). Additionally, the peak current was proportional to $[Hg^{2+}]$ in the range from 50 pM to 50 nM. The regression equation was I (μA) = −0.6591 + 0.4786 lg $[Hg^{2+}]$ (pM), R = 0.996. The detection limit of this Hg^{2+} electrochemical sensor was calculated to be 5 pM (details of the calculation of the detection limit are given in the SI), which was approximately 2 orders of magnitude lower than that of the colorimetric Hg^{2+} sensor. The linear range and detection limit of this electrochemical sensor were better than or at least comparable to those reported in the literature (SI, Table S1).

Moreover, satisfactory results confirmed the excellent selectivity of this electrochemical Hg^{2+} sensor (SI, Figure S7). Reproducibility of this Hg^{2+} electrochemical sensor was investigated by analyzing a 5 nM Hg^{2+} solution on five parallel prepared electrodes. The relative standard deviation of the values obtained from different electrodes was 6.9%. In addition, the prepared Hg^{2+} electrochemical sensor was tested after being stored at 4 °C for 1 week; in this case, 92.8% of the original signal remained, suggesting acceptable stability of the proposed biosensor. To test the applicability of the Ag-T sensing-units-

DOI: 10.1021/jacs.5b04348
J. Am. Chem. Soc. 2015, 137, 8880–8883

based electrochemical Hg^{2+} sensor, real water samples collected from tap water (Nanjing, China), well water (Wuxi, China), and lake water (Nanjing Xuanwu Lake, China) were tested. Certain amounts of Hg^{2+} ions were used to contaminate these water samples and the contaminated sample was subsequently tested by using the proposed electrochemical sensor and ICP-MS. The concentration and recovery of Hg^{2+} ions obtained by using our sensor were in good agreement with those obtained by using ICP-MS (Table 1), revealing the desirable applicability of Ag-T sensing units-based electrochemical method for Hg^{2+} determination.

Table 1. Hg^{2+} Determination Results Obtained by Using the Ag-T Sensing-Units-Based Electrochemical Hg^{2+} Sensor and ICP-MS of Real Water Samples

sample	Hg^{2+} spiked (nM)	ICP-MS (nM)	recovery (%)	proposed sensor (nM)	recovery (%)
lake water	0.00	1.32		1.29	
	2.50	3.91	104	3.66	94.8
	5.00	6.36	101	6.22	98.6
well water	0.00	–[a]		0.07	
	2.50	2.69	105	2.64	103
	5.00	5.11	102	5.05	99.6
tap water	0.00	–		0.08	
	2.50	2.75	110	2.42	93.6
	5.00	5.17	103	5.27	104

[a]– means "not detectable".

In summary, an approach has been proposed to convert a MN-based liquid-phase colorimetric assay into an enhanced surface-tethered electrochemical assay. By modifying the electrode surface with the same sensing elements used in MN-based colorimetric assays, target-induced MN aggregation was achieved on the electrode surface, resulting in the formation of the MN-based network architecture. The MN-based network architecture provided a well-defined and amplified electrochemical signal. Thus, a MN-based colorimetric assay was developed into a corresponding electrochemical assay with a significant improvement in sensitivity. This proof-of-concept study used the same principle and sensing units as a colorimetric sensor in a new electrochemical method for more sensitive Hg^{2+} detection. Taking advantage of the simple principle and easy operation of recent various MN-based colorimetric assays, this general approach is valuable in the design of very sensitive electrochemical sensors for practical use.

■ ASSOCIATED CONTENT

Supporting Information

Details of experiments and additional results. The Supporting Information is available free of charge on the ACS Publications website at DOI: 10.1021/jacs.5b04348.

■ AUTHOR INFORMATION

Corresponding Author

*daizhihuii@njnu.edu.cn

Notes

The authors declare no competing financial interest.

■ ACKNOWLEDGMENTS

This work was supported by NSFC (No. 21175069 and 21475062), Research Fund for the Doctoral Program of Higher Education of China (20113207110005) and Foundation of the Jiangsu Education Committee (11KJA150003) and Funding of Jiangsu Innovation Program for Graduate Education (KYZZ_0211). We appreciate the financial support from the Priority Academic Program Development of Jiangsu Higher Education Institutions.

■ REFERENCES

(1) Xia, F.; Zuo, X. L.; Yang, R. Q.; Xiao, Y.; Kang, D.; Vallee-Belisle, A.; Gong, X.; Yuen, J. D.; Hsu, B. B. Y.; Heeger, A. J.; Plaxco, K. W. *Proc. Natl. Acad. Sci. U. S. A.* **2010**, *107*, 10837−10841.

(2) Du, J. J.; Jiang, L.; Shao, Q.; Liu, X. G.; Marks, R. S.; Ma, J.; Chen, X. D. *Small* **2013**, *9*, 1467−1481.

(3) Kalluri, J. R.; Arbneshi, T.; Khan, S. A.; Neely, A.; Candice, P.; Varisli, B.; Washington, M.; McAfee, S.; Robinson, B.; Banerjee, S.; Singh, A. K.; Senapati, D.; Ray, P. C. *Angew. Chem., Int. Ed.* **2009**, *48*, 9668−9671.

(4) de la Rica, R.; Stevens, M. M. *Nat. Nanotechnol.* **2012**, *7*, 821−824.

(5) Rodriguez-Lorenzo, L.; de la Rica, R.; Alvarez-Puebla, R. A.; Liz-Marzan, L. M.; Stevens, M. M. *Nat. Mater.* **2012**, *11*, 604−607.

(6) Jiang, Y.; Zhao, H.; Lin, Y. Q.; Zhu, N. N.; Ma, Y. R.; Mao, L. Q. *Angew. Chem., Int. Ed.* **2010**, *49*, 4800−4804.

(7) Guo, L. H.; Xu, Y.; Ferhan, A. R.; Chen, G. N.; Kim, D. *J. Am. Chem. Soc.* **2013**, *135*, 12338−12345.

(8) Guo, Y. M.; Zhang, Y.; Shao, H. W.; Wang, Z.; Wang, X. F.; Jiang, X. Y. *Anal. Chem.* **2014**, *86*, 8530−8534.

(9) Ai, K. L.; Liu, Y. L.; Lu, L. H. *J. Am. Chem. Soc.* **2009**, *131*, 9496−9497.

(10) Tao, Y.; Lin, Y. H.; Ren, J. S.; Qu, X. G. *Biomaterials* **2013**, *34*, 4810−4817.

(11) Lee, S.; Manjunatha, D. H.; Jeon, W.; Ban, C. *PLoS One* **2014**, *9*, e100847.

(12) Lu, C. H.; Wang, Y. W.; Ye, S. L.; Chen, G. N.; Yang, H. H. *NPG Asia Mater.* **2012**, *4*, e10.

(13) Gao, T.; Ning, L. M.; Li, C.; Wang, H. Y.; Li, G. X. *Anal. Chim. Acta* **2013**, *788*, 171−176.

(14) Manley, M. *Chem. Soc. Rev.* **2014**, *43*, 8200−8214.

(15) Yeung, S. S. W.; Lee, T. M. H.; Hsing, I. M. *J. Am. Chem. Soc.* **2006**, *128*, 13374−13375.

(16) Wan, Y.; Zhou, Y. G.; Poudineh, M.; Safaei, T. S.; Mohamadi, R. M.; Sargent, E. H.; Kelley, S. O. *Angew. Chem., Int. Ed.* **2014**, *53*, 13145−13149.

(17) Toh, H. S.; Batchelor-McAuley, C.; Tschulik, K.; Uhlemann, M.; Crossley, A.; Compton, R. G. *Nanoscale* **2013**, *5*, 4884−4893.

(18) Xu, Q. N.; Yan, F.; Lei, J. P.; Leng, C.; Ju, H. X. *Chem. - Eur. J.* **2012**, *18*, 4994−4998.

(19) Korbas, M.; Blechinger, S. R.; Krone, P. H.; Pickering, I. J.; George, G. N. *Proc. Natl. Acad. Sci. U. S. A.* **2008**, *105*, 12108−12112.

(20) Xue, X. J.; Wang, F.; Liu, X. G. *J. Am. Chem. Soc.* **2008**, *130*, 3244−3245.

(21) Singh, P.; Parent, K. L.; Buttry, D. A. *J. Am. Chem. Soc.* **2012**, *134*, 5610−5617.

(22) Lim, D. K.; Jeon, K. S.; Hwang, J. H.; Kim, H.; Kwon, S.; Suh, Y. D.; Nam, J. M. *Nat. Nanotechnol.* **2011**, *6*, 452−460.

(23) Li, J.; Tu, W. W.; Li, H. B.; Han, M.; Lan, Y. Q.; Dai, Z. H.; Bao, J. C. *Anal. Chem.* **2014**, *86*, 1306−1312.

(24) Rassaei, L.; Marken, F.; Sillanpää, M.; Amiri, M.; Cirtiu, C. M.; Sillanpää, M. *TrAC, Trends Anal. Chem.* **2011**, *30*, 1704−1715.

(25) Zhou, Y. G.; Rees, N. V.; Compton, R. G. *Angew. Chem., Int. Ed.* **2011**, *50*, 4219−4221.

(26) Heiskanen, A. R.; Spegel, C. F.; Kostesha, N.; Ruzgas, T.; Emneus, J. *Langmuir* **2008**, *24*, 9066−9073.

DOI: 10.1021/jacs.5b04348
J. Am. Chem. Soc. 2015, 137, 8880−8883